A Greedy Algorithm for the Analysis Transform Domain

R. Giryes[a],[*]

[a] *The Department of Electrical and Computer Engineering, Duke University, Durham, NC 27708, USA*

Abstract

Many image processing applications benefited remarkably from the theory of sparsity. One model of sparsity is the cosparse analysis one. It was shown that using ℓ_1-minimization one might stably recover a cosparse signal from a small set of random linear measurements if the operator is a frame. Another effort has provided guarantees for dictionaries that have a near optimal projection procedure using greedy-like algorithms. However, no claims have been given for frames. A common drawback of all these existing techniques is their high computational cost for large dimensional problems.

In this work we propose a new greedy-like technique with theoretical recovery guarantees for frames as the analysis operator, closing the gap between greedy and relaxation techniques. Our results cover both the case of bounded adversarial noise, where we show that the algorithm provides us with a stable reconstruction, and the one of random Gaussian noise, for which we prove that it has a denoising effect, closing another gap in the analysis framework. Our proposed program, unlike the previous greedy-like ones that solely act in the signal domain, operates mainly in the analysis operator's transform domain. Besides the theoretical benefit, the main advantage of this strategy is its computational efficiency that makes it easily applicable to visually big data. We demonstrate its performance on several high dimensional images.

Keywords: Sparse representations, Compressed sensing, Sparsity for Big Data, Synthesis, Analysis, Iterative hard threshodling, Greedy Algorithms.
2010 MSC: 94A20, 94A12, 62H12

---

[*]Corresponding author

1. Introduction

For more than a decade the idea that signals may be represented sparsely has a great impact on the field of signal and image processing. New sampling theory has been developed [1] together with new tools for handling signals in different types of applications, such as image denoising [2], image deblurring [3], super-resolution [4], radar [5], medical imaging [6] and astronomy [7], to name a few [8]. Remarkably, in most of these fields the sparsity based techniques achieve state-of-the-art results.

The classical sparse model is the synthesis one. In this model the signal $\mathbf{x} \in \mathbb{R}^d$ is assumed to have a k-sparse representation $\boldsymbol{\alpha} \in \mathbb{R}^n$ under a given dictionary $\mathbf{D} \in \mathbb{R}^{d \times n}$. Formally,

$$\mathbf{x} = \mathbf{D}\boldsymbol{\alpha}, \quad \|\boldsymbol{\alpha}\|_0 \leq k, \tag{1}$$

where $\|\cdot\|_0$ is the ℓ_0-pseudo norm that counts the number of non-zero entries in a vector. Notice, that the non-zero elements in $\boldsymbol{\alpha}$ corresponds to a set of columns that creates a low-dimensional subspace in which $\mathbf{x}$ resides.

Recently, a new sparsity based model has been introduced: the analysis one [9, 10]. In this framework, we look at the coefficients of $\boldsymbol{\Omega}\mathbf{x}$, the coefficients of the signal after applying the transform $\boldsymbol{\Omega} \in \mathbb{R}^{p \times d}$ on it. The sparsity of the signal is measured by the number of zeros in $\boldsymbol{\Omega}\mathbf{x}$. We say that a signal is ℓ-cosparse if $\boldsymbol{\Omega}\mathbf{x}$ has ℓ zero elements. Formally,

$$\|\boldsymbol{\Omega}\mathbf{x}\|_0 \leq p - \ell. \tag{2}$$

Remark that each zero element in $\boldsymbol{\Omega}\mathbf{x}$ corresponds to a row in $\boldsymbol{\Omega}$ to which the signal is orthogonal and all these rows define a subspace to which the signal is orthogonal. Similar to synthesis, when the number of zeros is large the signal's subspace is low dimensional. Though the zeros are those that define the subspace, in some cases it is more convenient to use the number of non-zeros $k = p - \ell$ as done in [11, 12].

The main setup in which the above models have been used is

$$\mathbf{y} = \mathbf{M}\mathbf{x} + \mathbf{e}, \tag{3}$$

where $\mathbf{y} \in \mathbb{R}^m$ is a given set of measurements, $\mathbf{M} \in \mathbb{R}^{m \times d}$ is the measurement matrix and $\mathbf{e} \in \mathbb{R}^m$ is an additive noise which is assumed to be either adversarial bounded noise [1, 8, 13, 14] or with a certain given distribution such as Gaussian [15, 16, 17]. The goal is to recover $\mathbf{x}$ from $\mathbf{y}$ and this is the

2

focus of our work. For details about other setups, the curious reader may refer to [18, 19, 20, 21, 22, 23, 24].

Clearly, without a prior knowledge it is impossible to recover $\mathbf{x}$ from $\mathbf{y}$ in the case $m < d$, or have a significant denoising effect when $\mathbf{e}$ is random with a known distribution. Hence, having a prior, such as the sparsity one, is vital for these tasks. Both the synthesis and the analysis models lead to (different) minimization problems that provide estimates for the original signal $\mathbf{x}$.

In synthesis, the signal is recovered by its representation, using

$$\hat{\boldsymbol{\alpha}}_{S-\ell_0} = \operatorname*{argmin}_{\tilde{\boldsymbol{\alpha}} \in \mathbb{R}^n} \|\tilde{\boldsymbol{\alpha}}\|_0 \quad s.t \quad \|\mathbf{y} - \mathbf{MD}\tilde{\boldsymbol{\alpha}}\|_2 \leq \lambda_{\mathbf{e}}, \qquad (4)$$

where $\lambda_{\mathbf{e}}$ is an upper bound for $\|\mathbf{e}\|_2$ if the noise is bounded and adversarial ($S - \ell_0$ refers to synthesis-ℓ_0). Otherwise, it is a scalar dependent on the noise distribution [15, 16, 25]. The recovered signal is simply $\hat{\mathbf{x}}_{S-\ell_0} = \mathbf{D}\hat{\boldsymbol{\alpha}}_{S-\ell_0}$. In analysis, we have the following minimization problem.

$$\hat{\mathbf{x}}_{A-\ell_0} = \operatorname*{argmin}_{\tilde{\mathbf{x}} \in \mathbb{R}^d} \|\boldsymbol{\Omega}\tilde{\mathbf{x}}\|_0 \quad s.t \quad \|\mathbf{y} - \mathbf{M}\tilde{\mathbf{x}}\|_2 \leq \lambda_{\mathbf{e}}. \qquad (5)$$

The values of $\lambda_{\mathbf{e}}$ are selected as before depending on the noise properties ($A - \ell_0$ refers to analysis-ℓ_0).

Both (4) and (5) are NP-hard problems [10, 26]. Hence, approximation techniques are required. These are divided mainly into two categories: relaxation methods and greedy algorithms. In the first category we have the ℓ_1-relaxation [9] and the Dantzig selector [15], where the latter has been proposed only for synthesis. The ℓ_1-relaxation leads to the following minimization problems for synthesis and analysis respectively[1]:

$$\hat{\boldsymbol{\alpha}}_{S-\ell_1} = \operatorname*{argmin}_{\tilde{\boldsymbol{\alpha}} \in \mathbb{R}^n} \|\tilde{\boldsymbol{\alpha}}\|_1 \quad s.t \quad \|\mathbf{y} - \mathbf{MD}\tilde{\boldsymbol{\alpha}}\|_2 \leq \lambda_{\mathbf{e}}, \qquad (6)$$

$$\hat{\mathbf{x}}_{A-\ell_1} = \operatorname*{argmin}_{\tilde{\mathbf{x}} \in \mathbb{R}^d} \|\boldsymbol{\Omega}\tilde{\mathbf{x}}\|_1 \quad s.t \quad \|\mathbf{y} - \mathbf{M}\tilde{\mathbf{x}}\|_2 \leq \lambda_{\mathbf{e}}. \qquad (7)$$

Among the synthesis greedy strategies we mention the thresholding method, orthogonal matching pursuit (OMP) [30, 31, 32], CoSaMP [33], subspace pursuit (SP) [34], iterative hard thresholding [35] and hard thresholding pursuit (HTP) [36]. Their counterparts in analysis are thresholding [37], GAP [10],

---

[1]Note that setting $\boldsymbol{\Omega}$ to be the finite difference operator in (7) leads to the anisotropic version of the well-known total variation (TV) [27]. See [28, 29] for more details.

analysis CoSaMP (ACoSaMP), analysis SP (ASP), analysis IHT (AIHT) and analysis HTP (AHTP) [38].

An important question to ask is what are the recovery guarantees that exist for these methods. One main tool that was used for answering this question in the synthesis context is the restricted isometry property [13]. It has been shown that under some conditions on the RIP of $\mathbf{MD}$, we have in the adversarial bounded noise case that

$$\|\hat{\boldsymbol{\alpha}}_{alg} - \boldsymbol{\alpha}\|_2^2 \le C_{alg} \|\mathbf{e}\|_2^2, \tag{8}$$

where $\hat{\boldsymbol{\alpha}}_{alg}$ is the recovered representation by one of the approximation algorithms and $C_{alg} > 2$ is a constant that depends on the RIP of $\mathbf{MD}$ and differs for each of the methods [1, 13, 33, 34, 35, 36, 39, 40, 41]. This result implies that these programs achieve a stable recovery.

Similar results were provided for the case where the noise is random white Gaussian with variance σ^2 [15, 16, 17, 42]. In this case the reconstruction error is guaranteed to be $O(k \log(n)\sigma^2)$ [15, 16, 17]. Unlike the adversarial noise case, here we may have a denoising effect, as the recovery error can be smaller than the initial noise power $d\sigma^2$. Remark that the above results can be extended also to the case where we have a model mismatch and the signal is not exactly k-sparse.

In the analysis framework we have similar guarantees for the adversarial noise case. However, since the analysis model treats the signal directly, the guarantees are in terms of the signal and not the representation like in (8). Two extensions for the RIP have been proposed providing guarantees for analysis algorithms. The first is the D-RIP [11]:

Definition 1.1 (D-RIP [11]). *A matrix $\mathbf{M}$ has the D-RIP with a dictionary $\mathbf{D}$ and a constant $\delta_k = \delta_{\mathbf{D},k}$, if δ_k is the smallest constant that satisfies*

$$(1 - \delta_k) \|\mathbf{D}\tilde{\boldsymbol{\alpha}}\|_2^2 \le \|\mathbf{MD}\tilde{\boldsymbol{\alpha}}\|_2^2 \le (1 + \delta_k) \|\mathbf{D}\tilde{\boldsymbol{\alpha}}\|_2^2, \tag{9}$$

whenever $\tilde{\boldsymbol{\alpha}}$ is k-sparse.

The D-RIP has been used for studying the performance of the analysis ℓ_1-minimization [11, 43, 44]. It has been shown that if $\boldsymbol{\Omega}$ is a frame with frame constants A and B, $\mathbf{D} = \boldsymbol{\Omega}^\dagger$ and $\mathbf{M}$ has the D-RIP with $\delta_{ak} \le \delta_{A-\ell_1}(a, A, B)$ then

$$\|\hat{\mathbf{x}}_{A-\ell_1} - \mathbf{x}\|_2^2 \le C_{A-\ell_1} \left(\|\mathbf{e}\|_2^2 + \frac{\|\boldsymbol{\Omega}\mathbf{x} - [\boldsymbol{\Omega}\mathbf{x}]_k\|_1^2}{k} \right), \tag{10}$$

where the operator $[\cdot]_k$ is a hard thresholding operator that keeps the largest k elements in a vector, $\delta_{A-\ell_1}(a, A, B)$ is a function of a, A and B, and $a \geq 1$ and $C_{A-\ell_1}$ are some constants. A similar result has been proposed for analysis ℓ_1-minimization with the finite difference operator [28, 29].

The second is the O-RIP [38], which was used for the study of the greedy-like algorithms ACoSaMP, ASP, AIHT and AHTP.

Definition 1.2 (O-RIP [38]). *A matrix* $\mathbf{M}$ *has the O-RIP with an operator* $\mathbf{\Omega}$ *and a constant* $\delta_{\mathbf{\Omega},\ell}$, *if* $\delta_{\mathbf{\Omega},\ell}$ *is the smallest constant that satisfies*

$$(1 - \delta_{\mathbf{\Omega},\ell}) \|\mathbf{v}\|_2^2 \leq \|\mathbf{M}\mathbf{v}\|_2^2 \leq (1 + \delta_{\mathbf{\Omega},\ell}) \|\mathbf{v}\|_2^2, \tag{11}$$

whenever $\mathbf{\Omega}\mathbf{v}$ *has at least* ℓ *zeroes.*

With the assumption that there exists a cosupport selection procedure $\hat{\mathcal{S}}_\ell$ that implies a near optimal projection for $\mathbf{\Omega}$ with a constant C_ℓ (see Definition 3.1 in Section 3). It has been proven for such operators that if $\delta_{\mathbf{\Omega},a\ell} \leq \delta_{alg}(C_\ell, C_{2\ell-p}, \sigma_{\mathbf{M}}^2)$ then

$$\|\hat{\mathbf{x}}_{A-\ell_1} - \mathbf{x}\|_2^2 \leq C_{alg} \left(\|\mathbf{e}\|_2^2 + \left\| \mathbf{x} - \mathbf{x}^\ell \right\|_2^2 \right), \tag{12}$$

where $\sigma_{\mathbf{M}}^2$ is the largest singular value of $\mathbf{M}$, $\mathbf{x}^\ell$ is the best ℓ-cosparse approximation for $\mathbf{x}$, $\delta_{alg}(C_\ell, C_{2\ell-p}, \sigma_{\mathbf{M}}^2)$ is a function of C_ℓ, $C_{2\ell-p}$ and $\sigma_{\mathbf{M}}^2$, and $a \geq 3$ and C_{alg} are some constants that differ for each technique.

Notice that the conditions in synthesis imply that no linear dependencies can be allowed within small number of columns in the dictionary as the representation is the focus. The existence of such dependencies may cause ambiguity in its recovery. Since the analysis model performs in the signal domain, i.e. focus on the signal and not its representation, dependencies may be allowed within the dictionary. A recent series of contributions have shown that high correlations can be allowed in the dictionary also in the synthesis framework if the signal is the target and not the representation [45, 46, 47, 48, 49, 50, 51].

1.1. Our Contribution

The conditions for greedy-like techniques require the constant C_ℓ to be close to 1. Having a general projection scheme with $C_\ell = 1$ is NP-hard [52]. The existence of a program with a constant close to one for a general operator is still an open problem. In particular, it is not known whether

there exists a procedure that gives a small constant for frames. Thus, there is a gap between the results for the greedy techniques and the ones for the ℓ_1-minimization.

Another drawback of the existing analysis greedy strategies is their high complexity. All of them require applying a projection to an analysis cosparse subspace, which implies a high computational cost. Therefore, unlike in the synthesis case, they do not provide a "cheap" counterpart to the ℓ_1-minimization.

In this work we propose a new efficient greedy program, the transform domain IHT (TDIHT), which is an extension of IHT that operates in the analysis transform domain. Unlike AIHT, TDIHT has a low complexity, as it does not require applying computationally demanding projections like AIHT, and it inherits guarantees similar to the ones of analysis ℓ_1-minimization for frames. Given that $\mathbf{\Omega}$ and its pseudo-inverse $\mathbf{D}$ can be applied efficiently, TDIHT demands in each iteration applying only $\mathbf{\Omega}$, $\mathbf{D}$, the measurement matrix $\mathbf{M}$ and its transpose together with other point-wise operations. This puts TDIHT as an efficient alternative to the existing analysis methods especially for big data problems, as for high dimensional problems all the existing techniques require solving computationally demanding high dimensional optimization problems [10, 11, 38]. The assumption about $\mathbf{\Omega}$ and $\mathbf{D}$ holds for many types of operators such as curvelet, wavelets, Gabor transforms and discrete Fourier transform [11].

Another gap exists between synthesis and analysis. To the best of our knowledge, no denoising guarantees has been proposed for analysis strategies apart from the work in [37] that examines the performance of thresholding for the case $\mathbf{M} = \mathbf{I}$ and [53] that studies the analysis ℓ_0-minimization. We develop results for Gaussian noise in addition to the ones for adversarial noise, showing that it is possible to have a denoising effect using the analysis model also when $\mathbf{M} \neq \mathbf{I}$ and for different algorithms other than thresholding.

Our theoretical guarantees for TDIHT can be summarized by the following theorem:

Theorem 1.3 (Recovery Guarantees for TDIHT with Frames). *Let* $\mathbf{y} = \mathbf{Mx} + \mathbf{e}$ *where* $\|\mathbf{\Omega x}\|_0 \leq k$ *and* $\mathbf{\Omega}$ *is a frame with frame constants* A *and* B, *i.e.,* $\|\mathbf{\Omega}\|_2 \leq B$ *and* $\left\|\mathbf{\Omega}^\dagger\right\|_2 \leq \frac{1}{A}$. *For certain selections of* $\mathbf{M}$ *and using only*

6

$m = O(\frac{B}{A}k \log(p/k))$ *measurements, the recovery result $\hat{\mathbf{x}}$ of TDIHT satisfies*

$$\|\mathbf{x} - \hat{\mathbf{x}}\|_2 \leq O\left(\frac{B}{A}\|\mathbf{e}\|_2\right) \tag{13}$$
$$+O\left(\frac{1+A}{A^2}\|\mathbf{\Omega}_{T^C}\mathbf{x}\|_2 + \frac{1}{A^2\sqrt{k}}\|\mathbf{\Omega}_{T^C}\mathbf{x}\|_1\right),$$

for the case where $\mathbf{e}$ is an adversarial noise, implying that TDIHT leads to a stable recovery. For the case that $\mathbf{e}$ is random i.i.d zero-mean Gaussian distributed noise with a known variance σ^2 we have

$$E\|\mathbf{x} - \hat{\mathbf{x}}\|_2^2 \leq O\left(\frac{B^2}{A^2}k \log(p)\sigma^2\right) \tag{14}$$
$$+O\left(\frac{1+A}{A^2}\|\mathbf{\Omega}_{T^C}\mathbf{x}\|_2 + \frac{1}{A^2\sqrt{k}}\|\mathbf{\Omega}_{T^C}\mathbf{x}\|_1\right)^2,$$

implying that TDIHT achieves a denoising effect.

Remark 1.4. *Note that $\mathbf{\Omega}_{T^C}\mathbf{x} = \mathbf{\Omega}\mathbf{x} - [\mathbf{\Omega}\mathbf{x}]_k$.*

Remark 1.5. *Using Remark 2.3 in [33], we can convert the ℓ_2 norm into an ℓ_1 norm in the model mismatch terms in (13) and (14), turning it to be more similar to what we have in the bound for analysis ℓ_1-minimization in (10).*

Remark 1.6. *Theorem 1.3 is a combination of Theorems 4.1 and 4.4, plugging the minimal number of measurements implied by the D-RIP conditions of these theorems. Measurement matrices with sub-Gaussian entries are examples for matrices that satisfy this number of measurements [11].*

1.2. Organization

This paper is organized as follows. Section 2 includes the notations used in this paper together with some preliminary lemmas for the D-RIP. Section 3 presents the transform domain IHT. Section 4 provides the proof of our main theorem. In Section 5 we present some simulations demonstrating the efficiency of TDIHT and its applicability to big data. Section 6 concludes the paper.

2. Notations and Preliminaries

We use the following notation in our work:

- We denote by $\|\cdot\|_2$ the euclidean norm for vectors and the spectral $(2 \to 2)$ norm for matrices; by $\|\cdot\|_1$ the ℓ_1 norm that sums the absolute values of a vector; and by $\|\cdot\|_0$ the ℓ_0 pseudo-norm which counts the number of non-zero elements in a vector.

- Given a cosupport set Λ, $\boldsymbol{\Omega}_\Lambda$ is a sub-matrix of $\boldsymbol{\Omega}$ with the *rows* that belong to Λ.

- In a similar way, for a support set T, $\mathbf{D}_T$ is a sub-matrix of $\mathbf{D}$ with *columns*[2] corresponding to the set of indices in T.

- $(\mathbf{w})_T$ keeps the elements in $\mathbf{w}$ supported on T and zeros the rest.

- $\mathrm{supp}(\cdot)$ returns the support of a vector and $\mathrm{supp}(\cdot, k)$ returns the support set of k elements with largest magnitudes.

- $(\cdot)^\dagger$ denotes the Moore-Penrose pseudo-inverse [54].

- $\mathbf{Q}_\Lambda = \mathbf{I} - \boldsymbol{\Omega}_\Lambda^\dagger \boldsymbol{\Omega}_\Lambda$ is the orthogonal projection onto the orthogonal complement of $\mathrm{range}(\boldsymbol{\Omega}_\Lambda^*)$.

- $\mathbf{P}_T = \mathbf{D}_T \mathbf{D}_T^\dagger$ is the orthogonal projection onto $\mathrm{range}(\mathbf{D}_T)$.

- Throughout the paper we assume that $n = p$.

- The original unknown ℓ-cosparse vector is denoted by $\mathbf{x} \in \mathbb{R}^d$, its cosupport by Λ and the support of the non-zero entries by $T = \Lambda^C$. By definition $|\Lambda| \geq \ell$ and $|T| \leq k$.

- For a general ℓ-cosparse vector we use $\mathbf{v} \in \mathbb{R}^d$, for a general vector in the signal domain $\mathbf{z} \in \mathbb{R}^d$ and for a general vector in the analysis transform or dictionary representation domain $\mathbf{w} \in \mathbb{R}^p$.

---

[2]By the abuse of notation we use the same notation for the selection sub-matrices of rows and columns. The selection will be clear from the context since in analysis the focus is always on the rows and in synthesis on the columns.

We now turn to present several key properties of the D-RIP. All of their proofs except of the last one, which we present hereafter, appear in [50].

Corollary 2.1. *If* $\mathbf{M}$ *satisfies the D-RIP with a constant* δ_k *then*

$$\|\mathbf{M}\mathbf{P}_T\|_2^2 \leq 1 + \delta_k \tag{15}$$

for every T *such that* $|T| \leq k$.

Lemma 2.2. *For* $k \leq \tilde{k}$ *it holds that* $\delta_k \leq \delta_{\tilde{k}}$.

Lemma 2.3. *If* $\mathbf{M}$ *satisfies the D-RIP then*

$$\|\mathbf{P}_T(\mathbf{I} - \mathbf{M}^*\mathbf{M})\mathbf{P}_T\|_2 \leq \delta_k \tag{16}$$

for any T *such that* $|T| \leq k$.

Corollary 2.4. *If* $\mathbf{M}$ *satisfies the D-RIP then*

$$\|\mathbf{P}_{T_1}(\mathbf{I} - \mathbf{M}^*\mathbf{M})\mathbf{P}_{T_2}\|_2 \leq \delta_k, \tag{17}$$

for any T_1 *and* T_2 *such that* $|T_1| \leq k_1, |T_2| \leq k_2, k_1 + k_2 \leq k$.

The last Lemma we present is a generalization of Proposition 3.5 in [33].

Lemma 2.5. *Suppose that* $\mathbf{M}$ *satisfies the upper inequality of the D-RIP, i.e.,*

$$\|\mathbf{M}\mathbf{D}\mathbf{w}\|_2 \leq \sqrt{1 + \delta_k}\,\|\mathbf{D}\mathbf{w}\|_2 \qquad \forall \mathbf{w}, \|\mathbf{w}\|_0 \leq k, \tag{18}$$

and that $\|\mathbf{D}\|_2 \leq \frac{1}{A}$. *Then for any representation* $\mathbf{w}$ *we have*

$$\|\mathbf{M}\mathbf{D}\mathbf{w}\|_2 \leq \frac{\sqrt{1 + \delta_k}}{A}\left(\|\mathbf{w}\|_2 + \frac{1}{\sqrt{k}}\|\mathbf{w}\|_1\right). \tag{19}$$

The proof is left to Appendix Appendix A. Before we proceed we recall the problem we aim at solving:

Definition 2.6 (Problem $\mathcal{P}$). *Consider a measurement vector* $\mathbf{y} \in \mathbb{R}^m$ *such that* $\mathbf{y} = \mathbf{M}\mathbf{x} + \mathbf{e}$, *where* $\mathbf{x} \in \mathbb{R}^d$ *is either* ℓ-*cosparse under a given and fixed analysis operator* $\mathbf{\Omega} \in \mathbb{R}^{p \times d}$ *or almost* ℓ-*cosparse, i.e.* $\mathbf{\Omega}\mathbf{x}$ *has* $k = p - \ell$ *leading elements. The non-zero locations of the* k *leading elements is denoted by* T. $\mathbf{M} \in \mathbb{R}^{m \times d}$ *is a degradation operator and* $\mathbf{e} \in \mathbb{R}^m$ *is an additive noise. Our task is to recover* $\mathbf{x}$ *from* $\mathbf{y}$. *The recovery result is denoted by* $\hat{\mathbf{x}}$.

3. Transform Domain Iterative Hard Thresholding

Our goal in this section is to provide a greedy-like approach that provide guarantees similar to the one of analysis ℓ_1-minimization. By analyzing the latter we notice that though it operates directly on the signal, it actually minimizes the coefficients in the transform domain. In fact, all the proof techniques utilized for this recovery strategy use the fact that nearness in the analysis dictionary domain implies the same in the signal domain [11, 28, 43]. Using this fact, recovery guarantees have been developed for tight frames [11], general frames [43] and the 2D finite difference operator which corresponds to TV [28]. Working in the transform domain is not a new idea and was used before, especially in the context of dictionary learning [55, 56, 57].

Henceforth, our strategy for extending the results of the ℓ_1-relaxation is to modify the greedy-like approaches to operate in the transform domain. In this paper we concentrate on IHT. Before we turn to present the transform domain version of IHT we recall its synthesis and analysis versions.

3.1. Quick Review of IHT and AIHT

IHT and AIHT are assumed to know the cardinalities k and ℓ respectively. They aim at approximating variants of (4) and (5):

$$\operatorname*{argmin}_{\tilde{\boldsymbol{\alpha}}} \|\mathbf{y} - \mathbf{MD}\tilde{\boldsymbol{\alpha}}\|_2^2 \quad s.t. \quad \|\tilde{\boldsymbol{\alpha}}\|_0 \le k, \tag{20}$$

and

$$\operatorname*{argmin}_{\tilde{\mathbf{x}}} \|\mathbf{y} - \mathbf{M}\tilde{\mathbf{x}}\|_2^2 \quad s.t. \quad \|\boldsymbol{\Omega}\tilde{\mathbf{x}}\|_0 \le p - \ell. \tag{21}$$

IHT aims at recovering the representation and uses only one matrix $\mathbf{A} = \mathbf{MD}$ in the whole recovery process. AIHT targets the signal and utilizes both $\mathbf{M}$ and $\boldsymbol{\Omega}$. For recovering the signal using IHT, one has $\hat{\mathbf{x}}_{\text{IHT}} = \mathbf{D}\hat{\boldsymbol{\alpha}}_{\text{IHT}}$. IHT [35] and AIHT [38] are presented in Algorithms 1 and 2 respectively.

The iterations of IHT and AIHT are composed of two basic steps. In both of them the first is a gradient step, with a step size μ_t, in the direction of minimizing $\|\mathbf{y} - \mathbf{M}\tilde{\mathbf{x}}\|_2^2$. The second step of IHT projects $\boldsymbol{\alpha}_g$ to the closest k-sparse subspace by keeping the k elements with the largest magnitudes. In AIHT a cosupport selection procedure, $\mathcal{S}_\ell$, is used for the cosupport selection and then orthogonal projection onto the corresponding orthogonal subspace is performed. In the theoretical study of AIHT this procedure is assumed to apply a near optimal projection:

Definition 3.1. *A procedure $\hat{\mathcal{S}}_\ell$ implies a near-optimal projection $\mathbf{Q}_{\hat{\mathcal{S}}_\ell(\cdot)}$ with a constant C_ℓ if for any $\mathbf{z} \in \mathbb{R}^d$*

$$\left\| \mathbf{z} - \mathbf{Q}_{\hat{\mathcal{S}}_\ell(\mathbf{z})} \mathbf{z} \right\|_2^2 \le C_\ell \min_{\Lambda} \|\mathbf{z} - \mathbf{Q}_\Lambda \mathbf{z}\|_2^2. \tag{22}$$

More details about this definition can be found in [38].

In the algorithms' description we neither specify the stopping criterion, nor the step size selection technique. For exact details we refer the curious reader to [38, 35, 58, 59].

Algorithm 1 Iterative hard thresholding (IHT)

Require: $k, \mathbf{A}, \mathbf{y}$, where $\mathbf{y} = \mathbf{A}\boldsymbol{\alpha} + \mathbf{e}$, k is the cardinality of $\boldsymbol{\alpha}$ and $\mathbf{e}$ is an additive noise.
Ensure: $\hat{\boldsymbol{\alpha}}_{\mathrm{IHT}}$: k-sparse approximation of $\boldsymbol{\alpha}$.
  Initialize representation $\hat{\boldsymbol{\alpha}}^0 = \mathbf{0}$ and set $t = 0$.
  while halting criterion is not satisfied **do**
    $t = t + 1$.
    Perform a gradient step: $\boldsymbol{\alpha}_g = \hat{\boldsymbol{\alpha}}^{t-1} + \mu^t \mathbf{A}^*(\mathbf{y} - \mathbf{A}\hat{\boldsymbol{\alpha}}^{t-1})$
    Find a new support: $T^t = \mathrm{supp}(\boldsymbol{\alpha}_g, k)$
    Calculate a new representation: $\hat{\boldsymbol{\alpha}}^t = (\boldsymbol{\alpha}_g)_{T^t}$.
  end while
  Form the final solution $\hat{\boldsymbol{\alpha}}_{\mathrm{IHT}} = \hat{\boldsymbol{\alpha}}^t$.

Algorithm 2 Analysis iterative hard thresholding (AIHT)

Require: $\ell, \mathbf{M}, \Omega, \mathbf{y}$, where $\mathbf{y} = \mathbf{M}\mathbf{x} + \mathbf{e}$, ℓ is the cosparsity of $\mathbf{x}$ under Ω and $\mathbf{e}$ is an additive noise.
Ensure: $\hat{\mathbf{x}}_{\mathrm{AIHT}}$: ℓ-cosparse approximation of $\mathbf{x}$.
  Initialize estimate $\hat{\mathbf{x}}^0 = \mathbf{0}$ and set $t = 0$.
  while halting criterion is not satisfied **do**
    $t = t + 1$.
    Perform a gradient step: $\mathbf{x}_g = \hat{\mathbf{x}}^{t-1} + \mu^t \mathbf{M}^*(\mathbf{y} - \mathbf{M}\hat{\mathbf{x}}^{t-1})$
    Find a new cosupport: $\hat{\Lambda}^t = \hat{\mathcal{S}}_\ell(\mathbf{x}_g)$
    Calculate a new estimate: $\hat{\mathbf{x}}^t = \mathbf{Q}_{\hat{\Lambda}^t} \mathbf{x}_g$.
  end while
  Form the final solution $\hat{\mathbf{x}}_{\mathrm{AIHT}} = \hat{\mathbf{x}}^t$.

3.2. Transform Domain Analysis Greedy-Like Method

The drawback of AIHT for handling analysis signals is that it assumes the existence of a near optimal cosupport selection scheme $\mathcal{S}_\ell$. The type of analysis dictionaries for which a known feasible cosupport selection technique exists is very limited [38, 52]. Note that this limit is not unique only to the analysis framework [45, 46, 49]. Of course, it is possible to use a cosupport selection strategy with no guarantees on its near-optimality constant and it might work well in practice. For instance, simple hard thresholding has been shown to operate reasonably well in several instances where no practical projection is at hand [38]. However, the theoretical performance guarantees depend heavily on the near-optimality constant. Since for many operators there are no known selection schemes with small constants, the existing guarantees for AIHT, as well as the ones of the other greedy-like algorithms, are very limited. In particular, to date, they do not cover frames and the 2D finite difference operator as the analysis dictionary. Moreover, even when an efficient optimal selection procedure exists AIHT is required to apply a projection to the selected subspace which in many cases is computationally demanding.

To bypass these problems we propose an alternative greedy approach for the analysis framework that operates in the transform domain instead of the signal domain. This strategy aims at finding the closest approximation to $\mathbf{\Omega x}$ and not to $\mathbf{x}$ using the fact that for many analysis operators proximity in the transform domain implies the same in the signal domain. In some sense, this approach imitates the classical synthesis techniques that recover the signal by putting the representation as the target.

In Algorithm 3 an extension for IHT for the transform domain is proposed. This algorithm makes use of k, the number of non-zeros in $\mathbf{\Omega x}$, and $\mathbf{D}$, a dictionary satisfying $\mathbf{D\Omega} = \mathbf{I}$. One option for $\mathbf{D}$ is $\mathbf{D} = \mathbf{\Omega}^\dagger$. If $\mathbf{\Omega}$ does not have a full row rank, we may compute $\mathbf{D}$ by adding to $\mathbf{\Omega}$ rows that resides in its rows' null space and then applying the pseudo-inverse. For example, for the 2D finite difference operator we may calculate $\mathbf{D}$ by computing its pseudo inverse with an additional row composed of ones divided by $\sqrt{d}$. However, this option is not likely to provide good guarantees. As the 2D finite difference operator is beyond the scope of this paper we refer the reader to [28] for more details on this subject.

Indeed, for many operators $\mathbf{\Omega}$, there are infinitely many options for $\mathbf{D}$ such that $\mathbf{D\Omega} = \mathbf{I}$. When Algorithm 3 forms the final solution $\hat{\mathbf{x}}_{\text{TDIHT}} = \mathbf{D}\hat{\mathbf{w}}^t$, different choices of $\mathbf{D}$ will lead to different results since $\hat{\mathbf{w}}^t$ may not belong

12

to range$(\mathbf{\Omega})$. Therefore, in our study of the algorithm in the next section we focus on the choice of $\mathbf{\Omega}$ as a frame and $\mathbf{D} = \mathbf{\Omega}^\dagger$.

For the step size μ_t we can use several options. The first one it use a constant step size $\mu_t = \mu$ for all iterations. The second one is to use an 'optimal' step size that minimizes the fidelity term

$$\mu_t = \operatorname*{argmin}_{\mu} \left\| \mathbf{y} - \mathbf{M}\mathbf{D}\hat{\mathbf{w}}^t \right\|_2^2. \tag{23}$$

Since $\hat{\mathbf{w}}^t = (\mathbf{w}_g^t)_{\hat{T}^t}$ and $\hat{T}^t = \operatorname{supp}\left(\mathbf{\Omega}\mathbf{D}\hat{\mathbf{w}}^{t-1} + \mu^t\mathbf{\Omega}\mathbf{M}^*(\mathbf{y} - \mathbf{M}\mathbf{D}\hat{\mathbf{w}}^{t-1}), k\right)$ the above minimization problem does not have a close form solution and a line search for μ^t may involve a change of $\hat{T}^t$ several times. Instead, one may follow [58] and limits the minimization to the support $\tilde{T} = \hat{T}^{t-1} \cup \operatorname{supp}\left(\mathbf{\Omega}\mathbf{M}^*(\mathbf{y} - \mathbf{M}\mathbf{D}\hat{\mathbf{w}}^{t-1}), k\right)$. In this case we have

$$\begin{aligned}
\mu_t &= \operatorname*{argmin}_{\mu} \left\| \mathbf{y} - \mathbf{M}\mathbf{D}_{\tilde{T}}\mathbf{\Omega}_{\tilde{T}}\mathbf{D}\hat{\mathbf{w}}^{t-1} - \mu^t\mathbf{M}\mathbf{D}_{\tilde{T}}\mathbf{\Omega}_{\tilde{T}}\mathbf{M}^*(\mathbf{y} - \mathbf{M}\mathbf{D}\hat{\mathbf{w}}^{t-1}) \right\|_2^2 \quad (24) \\
&= \frac{(\mathbf{y} - \mathbf{M}\mathbf{D}_{\tilde{T}}\mathbf{\Omega}_{\tilde{T}}\mathbf{D}\hat{\mathbf{w}}^{t-1})^* \mathbf{M}\mathbf{D}_{\tilde{T}}\mathbf{\Omega}_{\tilde{T}}\mathbf{M}^*(\mathbf{y} - \mathbf{M}\mathbf{D}\hat{\mathbf{w}}^{t-1})}{\left\| \mathbf{M}\mathbf{D}_{\tilde{T}}\mathbf{\Omega}_{\tilde{T}}\mathbf{M}^*(\mathbf{y} - \mathbf{M}\mathbf{D}\hat{\mathbf{w}}^{t-1}) \right\|_2^2}.
\end{aligned}$$

We denote this selection technique as the adaptive changing step-size selection.

In this paper we focus in the theoretical part on TDIHT with $\mu = 1$. Our results can be easily extended also to the other step-size selection options using the proof techniques in [38, 58]. Naturally, TDIHT with an adaptive changing step-size selection behaves better than TDIHT with a constant μ. Therefore, in Section 5 we demonstrate the performance of the former.

4. Frame Guarantees

We provide theoretical guarantees for the reconstruction performance of the transform domain analysis IHT (TDIHT), with a constant step size $\mu = 1$, for frames. We start with the case that the noise is adversarial.

Theorem 4.1 (Stable Recovery of TDIHT with Frames). *Consider the problem $\mathcal{P}$ and apply TDIHT with a constant step-size $\mu = 1$ and $\mathbf{D} = \mathbf{\Omega}^\dagger$. Suppose that $\mathbf{e}$ is a bounded adversarial noise, $\mathbf{\Omega}$ is a frame with frame constants $0 < A, B < \infty$ such that $\|\mathbf{\Omega}\|_2 \leq B$ and $\|\mathbf{D}\|_2 \leq \frac{1}{A}$, and $\mathbf{M}$ has the D-RIP with the dictionary $[\mathbf{D}, \mathbf{\Omega}^*]$ and a constant $\delta_{\tilde{k}} = \delta_{[\mathbf{D}, \mathbf{\Omega}^*], \tilde{k}}^D$. If*

Algorithm 3 Transform Domain Iterative hard thresholding (TDIHT)

Require: $k, \mathbf{M} \in \mathbb{R}^{m \times d}, \mathbf{\Omega} \in \mathbb{R}^{p \times d}, \mathbf{D} \in \mathbb{R}^{d \times p}, \mathbf{y}$, where $\mathbf{y} = \mathbf{M}\mathbf{x} + \mathbf{e}$, $\mathbf{D}$ satisfies $\mathbf{D}\mathbf{\Omega} = \mathbf{I}$, $\mathbf{x}$ is $p - k$ cosparse under $\mathbf{\Omega}$ which implies that it has a k-sparse representation under $\mathbf{D}$, and $\mathbf{e}$ is an additive noise.
Ensure: $\hat{\mathbf{x}}_{\text{TDIHT}}$: Approximation of $\mathbf{x}$.
  Initialize estimate $\hat{\mathbf{w}}^0 = \mathbf{0}$ and set $t = 0$.
  while halting criterion is not satisfied **do**
    $t = t + 1$.
    Perform a gradient step: $\mathbf{w}_g^t = \mathbf{\Omega}\mathbf{D}\hat{\mathbf{w}}^{t-1} + \mu^t \mathbf{\Omega}\mathbf{M}^*(\mathbf{y} - \mathbf{M}\mathbf{D}\hat{\mathbf{w}}^{t-1})$
    Find a new transform domain support: $\hat{T}^t = \text{supp}(\mathbf{w}_g^t, k)$
    Calculate a new estimate: $\hat{\mathbf{w}}^t = (\mathbf{w}_g^t)_{\hat{T}^t}$.
  end while
  Form the final solution $\hat{\mathbf{x}}_{\text{TDIHT}} = \mathbf{D}\hat{\mathbf{w}}^t$.

$\rho \triangleq \frac{2\delta_{ak}B}{A} < 1$ *(i.e.* $\delta_{ak} \leq \frac{A}{2B}$*), then after a finite number of iterations* $t \geq t^* = \frac{\log\left((\sqrt{1+\delta_{2k}}B\|\mathbf{e}\|_2 + \eta)/\|\mathbf{\Omega}_T\mathbf{x}\|_2\right)}{\log(\rho)}$

$$\begin{aligned}
\left\|\mathbf{x} - \hat{\mathbf{x}}^t\right\|_2 \leq{}& \frac{2\eta}{A} + \frac{2B\sqrt{1+\delta_{2k}}}{A}\left(1 + \frac{1 - \rho^t}{1 - \rho}\right)\|\mathbf{e}\|_2 \qquad (25)\\
&+ \frac{2(1+\delta_{2k})}{A^2}\frac{1 - \rho^t}{1 - \rho}\Bigg(\left(1 + A + \frac{A^2}{2}\right)\|\mathbf{\Omega}_{T^C}\mathbf{x}\|_2\\
&\qquad\qquad\qquad\qquad\qquad + \frac{1}{\sqrt{k}}\|\mathbf{\Omega}_{T^C}\mathbf{x}\|_1\Bigg),
\end{aligned}$$

implying that TDIHT leads to a stable recovery. For tight frames $a = 3$ and for other frames $a = 4$.

The result of this theorem is a generalization of the one presented in [40] for IHT. Its proof follows from the following lemma.

Lemma 4.2. *Consider the same setup of Theorem 4.1. Then the t-th iteration of TDIHT satisfies*

$$\begin{aligned}
\left\|(\mathbf{\Omega}\mathbf{x} - \mathbf{w}_g^t)_{T \cup \hat{T}^t}\right\|_2 \leq{}& 2\delta_{ak}\frac{B}{A}\left\|(\mathbf{\Omega}\mathbf{x} - \mathbf{w}_g^{t-1})_{T \cup \hat{T}^{t-1}}\right\|_2 \qquad (26)\\
&+ \frac{1 + \delta_{2k}}{A}\left(\left(1 + A + \frac{A^2}{2}\right)\|\mathbf{\Omega}_{T^C}\mathbf{x}\|_2 + \frac{1}{\sqrt{k}}\|\mathbf{\Omega}_{T^C}\mathbf{x}\|_1\right)\\
&+ \|\mathbf{\Omega}_{T \cup \hat{T}^t}\mathbf{M}^*\mathbf{e}\|_2 .
\end{aligned}$$

14

The proof of the above lemma is left to Appendix Appendix A. We turn now to prove Theorem 4.1.

Proof:[Proof of Theorem 4.1] First notice that $\hat{\mathbf{w}}^0 = 0$ implies that $\mathbf{w}_g^0 = 0$. Using Lemma 4.2, recursion and the definitions of ρ and $T_{\mathbf{e}} \triangleq \text{argmax}_{\tilde{T}:|\tilde{T}| \leq k} \|\mathbf{\Omega}_{T \cup \tilde{T}} \mathbf{M}^* \mathbf{e}\|_2$, we have that after t iterations

$$\left\|(\mathbf{\Omega}\mathbf{x} - \mathbf{w}_g^t)_{T \cup \hat{T}^t}\right\|_2 \leq \rho^t \left\|(\mathbf{\Omega}\mathbf{x} - \mathbf{w}_g^0)_{T \cup \hat{T}^0}\right\|_2 \tag{27}$$

$$+ (1 + \rho + \rho^2 + \cdots + \rho^{t-1}) \left(\|\mathbf{\Omega}_{T \cup T_{\mathbf{e}}} \mathbf{M}^* \mathbf{e}\|_2 \right.$$

$$+ \frac{1 + \delta_{2k}}{A} \left((1 + A) \|\mathbf{\Omega}_{T^C} \mathbf{x}\|_2 + \frac{1}{\sqrt{k}} \|\mathbf{\Omega}_{T^C} \mathbf{x}\|_1 \right) \right)$$

$$= \rho^t \|\mathbf{\Omega}_T \mathbf{x}\|_2 + \frac{1 - \rho^t}{1 - \rho} \left(\|\mathbf{\Omega}_{T \cup T_{\mathbf{e}}} \mathbf{M}^* \mathbf{e}\|_2 + \right.$$

$$\frac{1 + \delta_{2k}}{A} \left((1 + A) \|\mathbf{\Omega}_{T^C} \mathbf{x}\|_2 + \frac{1}{\sqrt{k}} \|\mathbf{\Omega}_{T^C} \mathbf{x}\|_1 \right) \right),$$

where the last equality is due to the equation of geometric series ($\rho < 1$) and the facts that $\mathbf{w}_g^0 = 0$ and $T^0 = \emptyset$. For a given precision factor η we have that if $t \geq t^* = \frac{\log\left((\|\mathbf{\Omega}_{T \cup T_{\mathbf{e}}} \mathbf{M}^* \mathbf{e}\|_2 + \eta)/\|\mathbf{\Omega}_T \mathbf{x}\|_2\right)}{\log(\rho)}$ then

$$\rho^t \|\mathbf{\Omega}_T \mathbf{x}\|_2 \leq \eta + \|\mathbf{\Omega}_{T \cup T_{\mathbf{e}}} \mathbf{M}^* \mathbf{e}\|_2. \tag{28}$$

As $\mathbf{x} = \mathbf{D}\mathbf{\Omega}\mathbf{x}$ and $\hat{\mathbf{x}}^t = \mathbf{D}\hat{\mathbf{w}}^t$, we have using matrix norm inequality

$$\left\|\mathbf{x} - \hat{\mathbf{x}}^t\right\|_2 = \left\|\mathbf{D}(\mathbf{\Omega}\mathbf{x} - \hat{\mathbf{w}}^t)\right\|_2 \leq \frac{1}{A} \left\|\mathbf{\Omega}\mathbf{x} - \hat{\mathbf{w}}^t\right\|_2. \tag{29}$$

Using the triangle inequality and the facts that $\hat{\mathbf{w}}^t$ is supported on $\hat{T}^t$ and $\left\|\mathbf{\Omega}_{(T \cup \hat{T}^t)^C} \mathbf{x}\right\|_2 \leq \|\mathbf{\Omega}_{T^C} \mathbf{x}\|_2$, we have

$$\left\|\mathbf{x} - \hat{\mathbf{x}}^t\right\|_2 \leq \frac{1}{A} \|\mathbf{\Omega}_{T^C} \mathbf{x}\|_2 + \frac{1}{A} \left\|(\mathbf{\Omega}\mathbf{x} - \hat{\mathbf{w}}^t)_{T \cup \hat{T}^t}\right\|_2. \tag{30}$$

By using again the triangle inequality and the fact that $\hat{\mathbf{w}}^t$ is the best k-term approximation for $\mathbf{w}_g^t$ we get

$$
\begin{aligned}
\left\|\mathbf{x} - \hat{\mathbf{x}}^t\right\|_2 &\leq \frac{1}{A}\left\|\mathbf{\Omega}_{T^C}\mathbf{x}\right\|_2 + \frac{1}{A}\left\|(\mathbf{\Omega}\mathbf{x} - \mathbf{w}_g^t)_{T\cup\hat{T}^t}\right\|_2 \\
&\quad + \frac{1}{A}\left\|(\mathbf{w}_g^t - \hat{\mathbf{w}}^t)_{T\cup\hat{T}^t}\right\|_2 \\
&\leq \frac{1}{A}\left\|\mathbf{\Omega}_{T^C}\mathbf{x}\right\|_2 + \frac{2}{A}\left\|(\mathbf{\Omega}\mathbf{x} - \mathbf{w}_g^t)_{T\cup\hat{T}^t}\right\|_2 .
\end{aligned}
\tag{31}
$$

Plugging (28) and (27) in (31) yields

$$
\begin{aligned}
\left\|\mathbf{x} - \hat{\mathbf{x}}^t\right\|_2 &\leq \frac{2\eta}{A} + \frac{2}{A}\left(1 + \frac{1-\rho^t}{1-\rho}\right)\left\|\mathbf{\Omega}_{T\cup T_e}\mathbf{M}^*\mathbf{e}\right\|_2 \\
&\quad + \frac{2(1+\delta_{2k})}{A^2}\frac{1-\rho^t}{1-\rho}\left(\left(1 + A + \frac{A^2}{2}\right)\left\|\mathbf{\Omega}_{T^C}\mathbf{x}\right\|_2 \right. \\
&\qquad\qquad\qquad\qquad\qquad \left. + \frac{1}{\sqrt{k}}\left\|\mathbf{\Omega}_{T^C}\mathbf{x}\right\|_1\right).
\end{aligned}
\tag{32}
$$

Using the D-RIP and the fact that $\mathbf{\Omega}$ is a frame we have that $\|\mathbf{\Omega}_{T\cup T_e}\mathbf{M}^*\mathbf{e}\|_2 \leq B\sqrt{1+\delta_{2k}}\,\|\mathbf{e}\|_2$ and this completes the proof. $\qquad\square$

Having the result for the adversarial noise case we turn to give a bound for the case where a distribution of the noise is given. We dwell on the white Gaussian noise case. For this type of noise we make use of the following lemma.

Lemma 4.3. *If $\mathbf{e}$ is a zero-mean white Gaussian noise with a variance σ^2 then*

$$
E[\max_{|T|\leq k}\|\mathbf{\Omega}_T\mathbf{M}^*\mathbf{e}\|_2^2] \leq 4\max_i\|\mathbf{\Omega}_i^*\|_2^2(1+\delta_1)k\log(p)\sigma^2.
\tag{33}
$$

Proof: First notice that the i-th entry in $\mathbf{\Omega}_T\mathbf{M}^*\mathbf{e}$ is Gaussian distributed random variable with zero-mean and variance $\|\mathbf{M}\mathbf{\Omega}_i^*\|_2^2\sigma^2$. Denoting by $\mathbf{W}$ a diagonal matrix such that $\mathbf{W}_{i,i} = \|\mathbf{M}\mathbf{\Omega}_i^*\|_2$, we have that each entry in $\mathbf{W}^{-1}\mathbf{\Omega}_T\mathbf{M}^*\mathbf{e}$ is Gaussian distributed with variance σ^2. Therefore, using Theorem 2.4 from [17] we have $E[\max_{|T|\leq k}\|\mathbf{W}^{-1}\mathbf{\Omega}_T\mathbf{M}^*\mathbf{e}\|_2^2] \leq 4k\log(p)\sigma^2$. Using the D-RIP we have that $\|\mathbf{M}\mathbf{\Omega}_i^*\|_2^2 \leq (1+\delta_1)\|\mathbf{\Omega}_i^*\|_2^2$. Since the ℓ_2 matrix norm of a diagonal matrix is the maximal diagonal element we have that $\|\mathbf{W}\|_2^2 \leq \max_i(1+\delta_1)\|\mathbf{\Omega}_i^*\|_2^2$ and this provides the desired result. $\qquad\square$

Theorem 4.4 (Denoising Performance of TDIHT with Frames). *Consider the problem $\mathcal{P}$ and apply TDIHT with a constant step-size $\mu = 1$. Suppose that $\mathbf{e}$ is an additive white Gaussian noise with a known variance σ^2 (i.e. for each element $\mathbf{e}_i \sim N(0, \sigma^2)$), $\boldsymbol{\Omega}$ is a frame with frame constants $0 < A, B < \infty$ such that $\|\boldsymbol{\Omega}\|_2 \leq B$ and $\|\mathbf{D}\|_2 \leq \frac{1}{A}$, and $\mathbf{M}$ has the D-RIP with the dictionary $[\mathbf{D}, \boldsymbol{\Omega}^*]$ and a constant $\delta_{\tilde{k}} = \delta^D_{[\mathbf{D},\boldsymbol{\Omega}^*],\tilde{k}}$. If $\rho \triangleq \frac{2\delta_{ak}B}{A} < 1$ (i.e. $\delta_{ak} \leq \frac{A}{2B}$), then after a finite number of iterations $t \geq t^* = \frac{\log\left((\|\boldsymbol{\Omega}_{T \cup T_{\mathbf{e}}}\mathbf{M}^*\mathbf{e}\|_2 + \eta)/\|\boldsymbol{\Omega}_T \mathbf{x}\|_2\right)}{\log(\rho)}$*

$$E\left\|\mathbf{x} - \hat{\mathbf{x}}^t\right\|_2^2 \leq \frac{32(1+\delta_1)B^2}{A^2}\left(1 + \frac{1-\rho^t}{1-\rho}\right)^2 k \log(p)\sigma^2 \tag{34}$$

$$+\frac{8(1+\delta_{2k})^2}{A^4}\left(\frac{1-\rho^t}{1-\rho}\right)^2\left(\left(1 + A + \frac{A^2}{2}\right)\|\boldsymbol{\Omega}_{T^C}\mathbf{x}\|_2\right.$$

$$\left.+ \frac{1}{\sqrt{k}}\|\boldsymbol{\Omega}_{T^C}\mathbf{x}\|_1\right)^2,$$

implying that TDIHT has a denoising effect. For tight frames $a = 3$ and for other frames $a = 4$.

Proof: Using the fact that for tight frames $\max_i \|\boldsymbol{\Omega}_i^*\|_2^2 \leq B$, we have using Lemma 4.3 that

$$E\left\|\boldsymbol{\Omega}_{T \cup T_{\mathbf{e}}}\mathbf{M}^*\mathbf{e}\right\|_2^2 \leq 4B^2(1+\delta_1)k\log(p)\sigma^2. \tag{35}$$

Plugging this in a squared version of (32) (with $\eta = 0$), using the fact that for any two constants a, b we have $(a+b)^2 \leq 2a^2 + 2b^2$, leads to the desired result. $\square$

4.1. Result's Optimality

Notice that in all our conditions, the number of measurements we need is $O((p - \ell)\log(p))$ and it is not dependent explicitly on the intrinsic dimension of the signal. Intuitively, we would expect the minimal number of measurements to be rather a function of $d - r$, where $r = \text{rank}(\boldsymbol{\Omega}_\Lambda)$ (refer to [10, 38] for more details), and henceforth our recovery conditions seems to be sub-optimal.

Indeed, this is the case with the analysis ℓ_0-minimization problem [10]. However, all the guarantees developed for feasible programs [11, 38, 28, 43, 44]

require at least $O((p - \ell)\log(p/(p - \ell)))$ measurements. Apparently, such conditions are too demanding because $d - r$, which can be much smaller than $p - \ell$, does not play any role in them. However, it seems that it is impossible to robustly reconstruct the signal with fewer measurements [53].

The same argument may be used for the denoising bound we have for TDIHT $(O((p - \ell)\log(p)\sigma^2))$, saying that we would expect it to be $O((d - r)\log(p)\sigma^2)$. Interestingly, even the ℓ_0 solution cannot achieve the latter bound but only a one which is a function of the cosparsity [53].

In this work we developed recovery guarantees for TDIHT with frames. These guarantees close a gap between relaxation-based techniques and greedy algorithms in the analysis framework, and extend the denoising guarantees of synthesis methods to analysis. It is interesting to ask whether these can be extended to other operators such as the 2D finite difference or to other methods such as AIHT or an analysis version of the Dantzig selector. The core idea in this work is the connection between the signal domain and the transform domain. We believe that the relationships used in this work can be developed further, leading to other new results and improving existing techniques. Some results in this direction appear in [29].

5. Experiments

In this section we repeat some of the experiments performed in [10, 38, 60]. We start with synthetic signals in the noiseless case. We test the performance of TDIHT with an adaptive changing step-size and compare it with AIHT, AHTP, ASP, ACoSaMP [38], ℓ_1-minimization [9] and GAP [10]. As there are several possibilities for setting the parameters in AIHT, AHTP, ASP and ACoSaMP we select the ones that provide the best performance according to [38].

We draw a phase transition diagram [61] for each of the algorithms. We use a random matrix $\mathbf{M}$ and a random tight frame $\mathbf{\Omega}$ with $d = 120$ and $p = 144$, where each entry in the matrices is drawn independently from the Gaussian distribution. We test 20 different possible values of m and 20 different values of ℓ and for each pair repeat the experiment 50 times. In each experiment we check whether we have a perfect reconstruction. White cells in the diagram denote a perfect reconstruction in all the experiments of the pair and black cells denotes total failure in the reconstruction. The values of m and ℓ are selected according to the following formula:

$$m = \delta d \qquad \ell = d - \rho m, \tag{36}$$

18

(a) AIHT, adaptive step-size

(b) AHTP, adaptive step-size

(c) ACoSaMP

(d) ASP

(e) TDIHT, adaptive step-size


(f) A-ℓ_1-minimization

(g) GAP
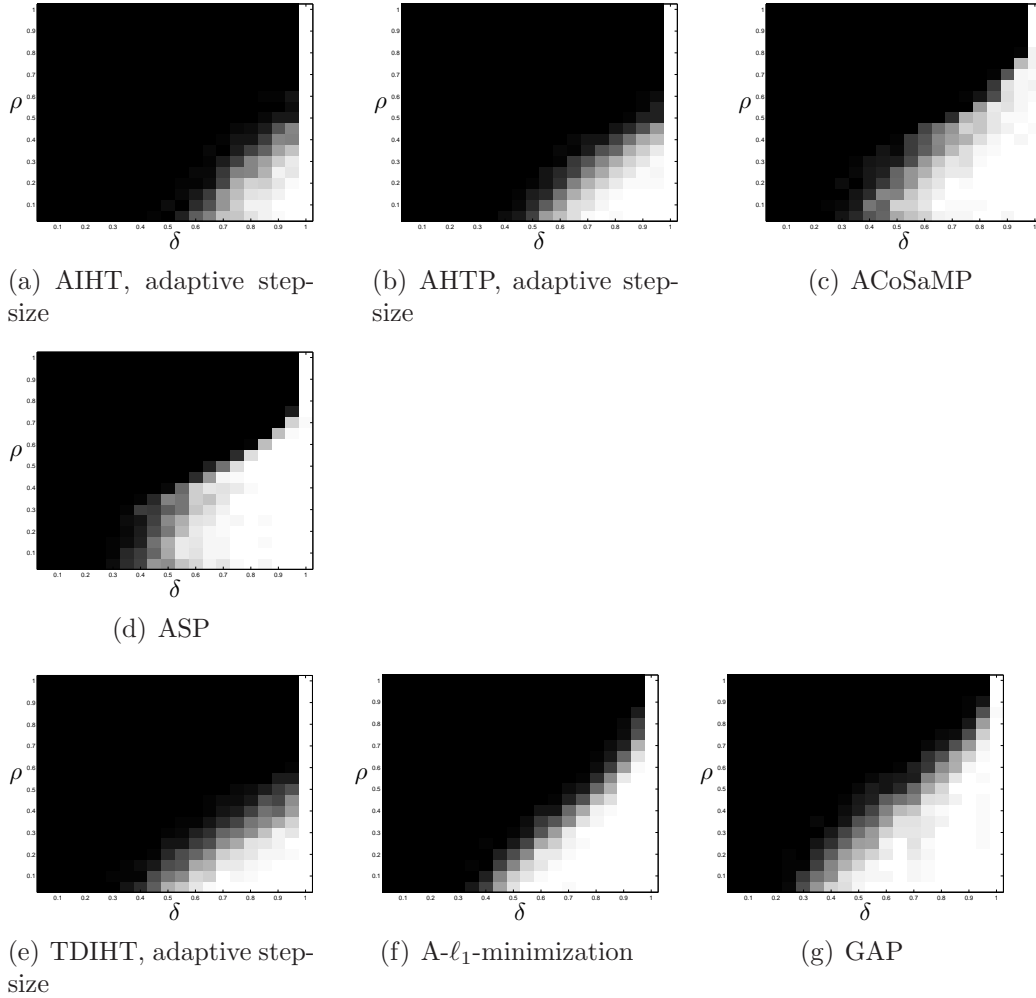
Figure 1: Recovery rate for a random tight frame with $p = 144$ and $d = 120$. From left to right, up to bottom: AIHT with an adaptive changing step-size, AHTP with an adaptive changing step-size, ACoSaMP, ASP, TDIHT with an adaptive changing step-size, A-ℓ_1-minimization and GAP.

where δ, the sampling rate, is the x-axis of the phase diagram and ρ, the ratio between the cosparsity of the signal and the number of measurements, is the y-axis.

Figure 1 compares the reconstruction results of TDIHT with an adaptive changing step-size with the other algorithms. It should be observed that TDIHT outperforms AIHT and provides comparable results with AHTP,

19

(a) Shepp-Logan phantom

(b) FLAIT brain

(c) Lumbar spine

(d) Circle of Willis
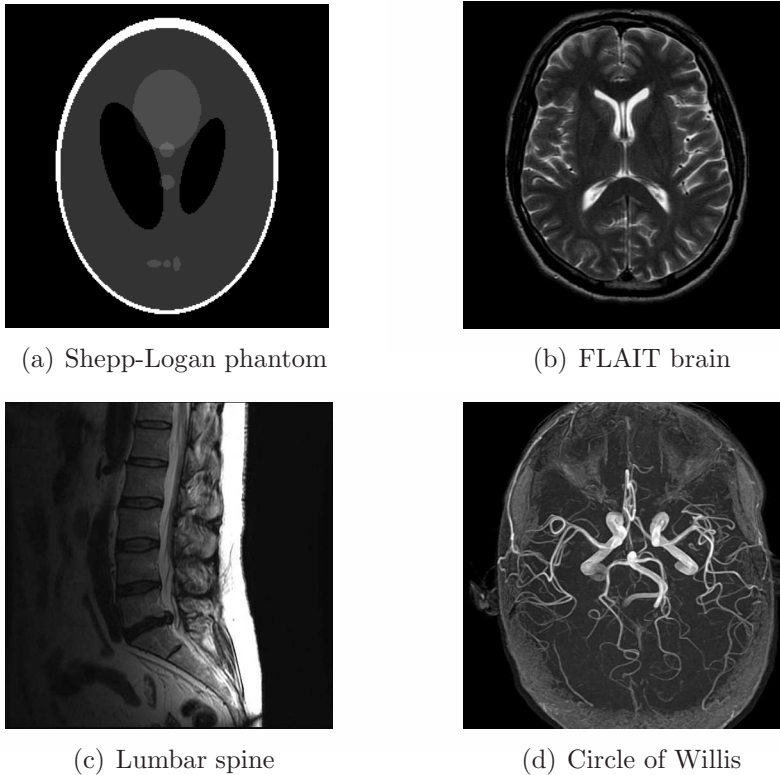
Figure 2: Test Images.

where TDIHT is more computationally efficient than both of them. Though its performance is inferior to the other algorithms, it should be noted that its running time is faster by one order of magnitude compared to all the other techniques. Therefore, in the cases that it succeeds, it should be favored over the other programs due to its better running time.

We turn now to test TDIHT for high dimensional signals. We test the performance of several MRI images: the *Shepp-Logan phantom*, *FLAIT brain* image, T2 Sagittal view of the *lumbar spine* and the *circle of Willis*. The first image is of size 256×256, while the other are of size 512×512. They are all presented in Fig. 2.

We focus on the recovery of these images from a few number of Fourier measurements. With $\mathbf{\Omega}$ set to be the undecimated Haar transform with one level of resolution (redundancy four) and $\mathbf{D}$ its inverse transform, we succeed to recover the phantom image using only 18 sampled radial lines, which is

(a) Naive PSNR $= 18.3dB$ (b) TDIHT PSNR $= 36dB$
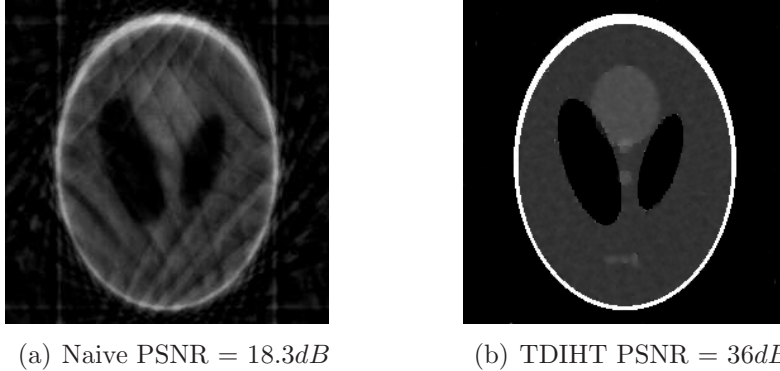
Figure 3: Recovery of the Shepp-Logan phantom from noisy 28 radial lines with SNR of 20. From left to right: Naive and TDIHT recovery. Note that for the noiseless case TDIHT gets a perfect reconstruction using only 18 radial lines.

only 6.5% of the measurements. This number is only slightly larger than the number needed for GAP, relaxed ASP (RASP) and Relaxed ACoSaMP (RACoSaMP) in [10, 38]. The advantage of TDIHT over these methods is its low complexity as it requires applying only $\mathbf{M}$ and its conjugate and $\mathbf{\Omega}$ and its inverse transform while in the other algorithms a high dimensional least squares minimization problem should be solved. Note also that for AIHT and RAHTP the number of radial lines needed for recovery is 35 and for IHT (with the decimated Haar operator with one level of resolution) we need more than 50 radial lines.

Exploring the noisy case, we perform a reconstruction using TDIHT of a noisy measurement of the phantom with 28 radial lines and signal to noise ratio (SNR) of 20. Figure 3(a) presents the naive recovery from noisy image, the result of applying inverse Fourier transform on the measurements with zero-padding, and Fig. 3(b) presents the TDIHT reconstruction result. We get a peak SNR (PSNR) of $36dB$. Note that RASP and GAPN require 22 radial lines to get the same PSNR. However, this comes at the cost of higher computational complexity.

We perform similar experiments for the other images. Instead of uniformly sampling radial lines, we use pseudo-random variable-density undersampling patterns [62][3] presented in Fig. 4. We use var. dens. 1 with FLAIT

_____

[3]Unlike [62] we perform our experiments with real (non-complex) images. The sampling

(a) Var. dens. 1   (b) Var. dens. 2
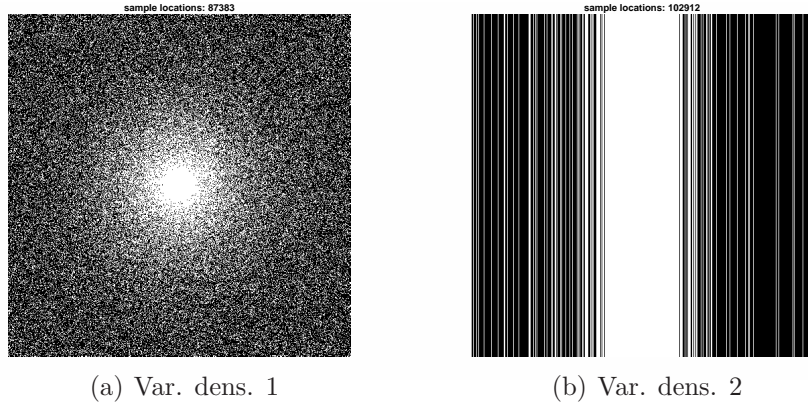
Figure 4: Pseudo-random variable-density undersampling patterns.

Method	FLAIT Brain		Lumber Spine		The Circle of Willis	
	Noiseless	Noisy	Noiseless	Noisy	Noiseless	Noisy
Naive	31.7	31.3	34.5	33.3	30	29.6
TDIHT	43.9	39.2	42.2	36.6	38.2	34.8
RASP	41.3	36.2	39.9	36.5	34.3	33.2
GAP	42.1	35.8	40.4	34.6	36.2	32.7

Table 1: Recovery of FLAIT brain from var. dens. 1 samples, lumber spine from var. dens. 2 samples and circle of Willis from var. dens. 1 samples in the noiseless and noisy (with SNR 20) cases. The reconstruction quality is measured by PSNR.

brain and the circle of Willis and var. dens. 2 with lumber spine.

As the images at hand are only approximately cosparse, we set a threshold, 0.01 in the noiseless case and 0.05 in the noisy one, such that each element in the cosparse representation below it is considered as zero. These thresholds create a model error in the recovery but provide a larger cosparsity value that eases the recovery. Moreover, in the noisy case, it is natural to set such a threshold since anyway small representation coefficients are being covered by the noise.

Table 1 summarizes the recovery performance, in terms of PSNR, for the FLAIT brain, lumbar spine and circle of Willis images both for the

---

patterns we use can be downloaded from *http://www.eecs.berkeley.edu/∼mlustig/CS.html*.
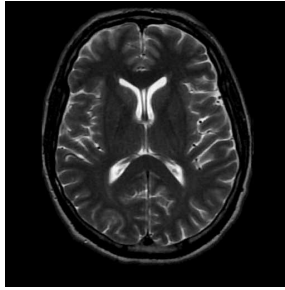
(a) TDIHT PSNR = 39.2dB
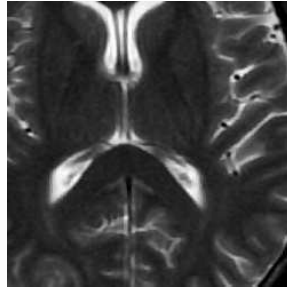
(b) TDIHT zoom in
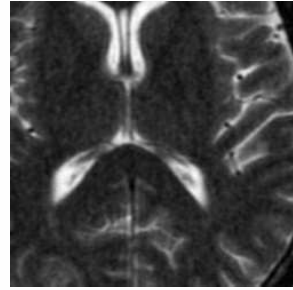
(c) Naive zoom in. PSNR = 31.3dB

(d) TDIHT PSNR 36.6dB
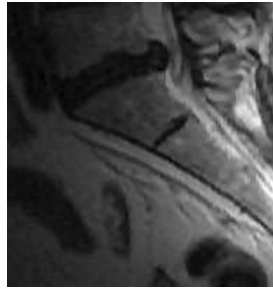
(e) TDIHT zoom in
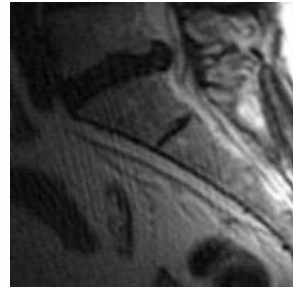
(f) Naive zoom in. PSNR = 33.3dB
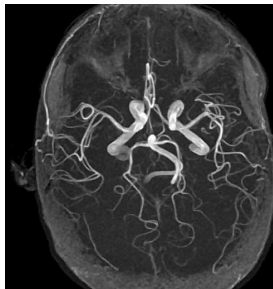
(g) TDIHT PSNR 34.8dB

(h) TDIHT zoom in
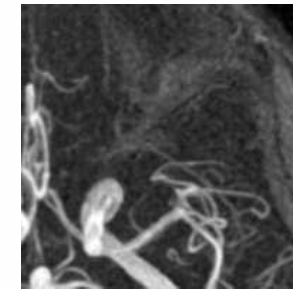
(i) Naive zoom in. PSNR = 29.6dB

Figure 5: Reconstruction from noisy measurements with SNR 20. From left to right: TDIHT recovery, zoom-in on TDIHT recovery and zoom-in on naive recovery. From top to bottom: Recovery of FLAIT brain from var. dens. 1 samples, lumber spine from var. dens. 2 samples and circle of Willis from var. dens. 1. samples.

noiseless and noisy cases. To evaluate the performance of TDIHT in the noiseless case, we compare its PSNR with the one of the model error (which we get by applying $\mathbf{\Omega}$ on the original image followed by thresholding and multiplication by $\mathbf{D}$). For FLAIT brain and lumber spine we get errors, which are comparable, and even better for the latter, to their model errors $44.5dB$ and $44dB$. Note that such high PSNRs are equivalent to mean squared errors of the order of 10^{-5} and therefore we may say that we achieve a perfect recovery in these cases. This is not the case for the circle of Willis, in which the error is worse than the model error $41.3dB$. Note though that for this image, as well as for the other two images, we get better recovery error than the more sophisticated methods RASP and GAP. Even in the noisy case, the quality we get with TDIHT is better than the one we have using those methods.

Figs. 5 presents the reconstruction outcome of TDIHT in the noisy case. To illustrate better the recovery gain, we present a zoom in on a part of the image and compare it to the naive recovery. The improvement can be seen clearly in all the three images.

6. Conclusion

This paper presents a new algorithm, the transform domain IHT (TDIHT), for the cosparse analysis framework. In contrast to previous algorithms, TDIHT can be applied efficiently in high dimensional problems due to the fact that it requires applying only the measurement matrix $\mathbf{M}$, its transpose $\mathbf{M}^*$, the operator $\mathbf{\Omega}$ and its inverse $\mathbf{D}$ together with point-wise operations. The proposed algorithm is shown to provide stable recovery given that $\mathbf{M}$ has the D-RIP and that $\mathbf{\Omega}$ is a frame. One of the limits of the proposed algorithm is that it assumes that the inverse of $\mathbf{\Omega}$ is given and can be easily applied in high dimensional problems. Though this is true for many types of operators like the discrete Fourier transform, wavelets and the Gabor frames [11], it is not always possible to apply the inverse efficiently and there are even examples for operators for which such an inverse does not even exist, e.g., the finite difference operator [28]. A future work should pursue an efficient algorithm adapted to this case.

Appendix A. Proof of Lemma 2.5

Lemma 2.5. Suppose that $\mathbf{M}$ satisfies the upper inequality of the D-RIP, i.e.,

$$\|\mathbf{MDw}\|_2 \leq \sqrt{1 + \delta_k}\, \|\mathbf{Dw}\|_2 \qquad \forall \mathbf{w}, \|\mathbf{w}\|_0 \leq k, \tag{A.1}$$

and that $\|\mathbf{D}\|_2 \leq \frac{1}{A}$. Then for any representation $\mathbf{w}$ we have

$$\|\mathbf{MDw}\|_2 \leq \frac{\sqrt{1 + \delta_k}}{A} \left(\|\mathbf{w}\|_2 + \frac{1}{\sqrt{k}} \|\mathbf{w}\|_1 \right). \tag{A.2}$$

Proof: We follow the proof of Proposition 3.5 in [33]. We define the following two convex bodies

$$S = \operatorname{conv}\left\{ \mathbf{Dw} : \mathbf{w}_{T^C} = 0, |T| \leq k, \|\mathbf{Dw}\|_2 \leq 1 \right\}, \tag{A.3}$$

$$K = \left\{ \mathbf{Dw} : \frac{1}{A}\left(\|\mathbf{w}\|_2 + \frac{1}{\sqrt{k}} \|\mathbf{w}\|_1 \right) \leq 1 \right\}. \tag{A.4}$$

Since

$$\|\mathbf{M}\|_{S \to 2} = \max_{\mathbf{v} \in S} \|\mathbf{Mv}\|_2 \leq \sqrt{1 + \delta_k}, \tag{A.5}$$

it is sufficient to show that $\|\mathbf{M}\|_{K \to 2} = \max_{\mathbf{v} \in K} \|\mathbf{Mv}\|_2 \leq \|\mathbf{M}\|_{S \to 2}$ which holds if $K \subset S$. For proving the latter, let $\mathbf{Dw} \in K$ and $\{T_0, T_1, \ldots, T_J\}$ be a set of distinct sets such that T_0 is composed of the indexes of the k-largest entries in $\mathbf{w}$, T_1 of the next k-largest entries, and so on. Thus, we can rewrite $\mathbf{Dw} = \sum_{i=0}^{J} \mathbf{Dw}_{T_i} = \sum_{i=0}^{J} \lambda_i \mathbf{D\tilde{w}}_{T_i}$, where $\lambda_i = \|\mathbf{Dw}_{T_i}\|_2$ and $\tilde{\mathbf{w}}_{T_i} = \mathbf{w}_{T_i}/\lambda_i$. Notice that by definition $\mathbf{D\tilde{w}}_{T_i} \in S$. It remains to show that $\sum_{i=0}^{J} \lambda_i \leq 1$ in order to show that $\mathbf{Dw} \in S$. It is easy to show that $\|\mathbf{w}_{T_i}\|_2 \leq \frac{\|\mathbf{w}_{T_{i-1}}\|_1}{\sqrt{k}}$. Combining this with the fact that $\|\mathbf{D}\|_2 \leq \frac{1}{A}$ leads to

$$\begin{aligned}
\sum_{i=1}^{J} \lambda_i &= \sum_{i=1}^{J} \|\mathbf{Dw}_{T_i}\|_2 \leq \frac{1}{A} \sum_{i=1}^{J} \|\mathbf{w}_{T_i}\|_2 \\
&\leq \frac{1}{A\sqrt{k}} \sum_{i=0}^{J-1} \|\mathbf{w}_{T_i}\|_1 \leq \frac{1}{A\sqrt{k}} \|\mathbf{w}\|_1.
\end{aligned} \tag{A.6}$$

Using the fact that $\lambda_0 = \|\mathbf{D}\mathbf{w}_{T_0}\|_2 \leq \frac{1}{A}\|\mathbf{w}_{T_0}\|_2 \leq \frac{1}{A}\|\mathbf{w}\|_2$, we have

$$\sum_{i=0}^{J}\lambda_i \leq \frac{1}{A}\left(\|\mathbf{w}\|_2 + \frac{1}{\sqrt{k}}\|\mathbf{w}\|_1\right) \leq 1, \tag{A.7}$$

where the last inequality is due to the fact that $\mathbf{D}\mathbf{w} \in K$. $\qquad\square$

Appendix A. Proof of Lemma 4.2

Lemma 4.2. Consider the same setup of Theorem 4.1. Then the t-th iteration of TDIHT satisfies

$$\left\|\left(\mathbf{\Omega}\mathbf{x} - \mathbf{w}_g^t\right)_{T\cup\hat{T}^t}\right\|_2 \leq 2\delta_{ak}\frac{B}{A}\left\|\left(\mathbf{\Omega}\mathbf{x} - \mathbf{w}_g^{t-1}\right)_{T\cup\hat{T}^{t-1}}\right\|_2 \tag{A.1}$$

$$+\frac{1+\delta_{2k}}{A}\left(\left(1 + A + \frac{A^2}{2}\right)\|\mathbf{\Omega}_{T^C}\mathbf{x}\|_2 + \frac{1}{\sqrt{k}}\|\mathbf{\Omega}_{T^C}\mathbf{x}\|_1\right)$$

$$+\|\mathbf{\Omega}_{T\cup\hat{T}^t}\mathbf{M}^*\mathbf{e}\|_2.$$

Proof: Our proof technique is based on the one of IHT in [40], utilizing the properties of $\mathbf{\Omega}$ and $\mathbf{D}$. Denoting $\mathbf{w} = \mathbf{\Omega}\mathbf{x}$ and using the fact that $\mathbf{w}_g^t = \mathbf{\Omega}\mathbf{D}\hat{\mathbf{w}}^{t-1} - \mathbf{\Omega}\mathbf{M}^*(\mathbf{y} - \mathbf{M}\mathbf{D}\hat{\mathbf{w}}^{t-1})$ we have

$$\left\|\left(\mathbf{w} - \mathbf{w}_g^t\right)_{T\cup\hat{T}^t}\right\|_2 = \tag{A.2}$$

$$\left\|\left(\mathbf{w} - \mathbf{\Omega}\mathbf{D}\hat{\mathbf{w}}^{t-1}\right)_{T\cup\hat{T}^t} - \left(\mathbf{\Omega}\mathbf{M}^*(\mathbf{y} - \mathbf{M}\mathbf{D}\hat{\mathbf{w}}^{t-1})\right)_{T\cup\hat{T}^t}\right\|_2.$$

By definition $\mathbf{w} = \mathbf{\Omega}\mathbf{D}\mathbf{w}$ and $\mathbf{y} = \mathbf{M}\mathbf{D}\mathbf{w} + \mathbf{e}$. Henceforth

$$\left\|\left(\mathbf{w} - \mathbf{w}_g^t\right)_{T\cup\hat{T}^t}\right\|_2 \tag{A.3}$$

$$= \left\|\mathbf{\Omega}_{T\cup\hat{T}^t}\mathbf{D}\left(\mathbf{w} - \hat{\mathbf{w}}^{t-1}\right) - \mathbf{\Omega}_{T\cup\hat{T}^t}\mathbf{M}^*(\mathbf{y} - \mathbf{M}\mathbf{D}\hat{\mathbf{w}}^{t-1})\right\|_2$$

$$= \left\|\mathbf{\Omega}_{T\cup\hat{T}^t}(\mathbf{I} - \mathbf{M}^*\mathbf{M})\mathbf{D}\left(\mathbf{w} - \hat{\mathbf{w}}^{t-1}\right) - \mathbf{\Omega}_{T\cup\hat{T}^t}\mathbf{M}^*\mathbf{e}\right\|_2$$

$$\leq \left\|\mathbf{\Omega}_{T\cup\hat{T}^t}(\mathbf{I} - \mathbf{M}^*\mathbf{M})\mathbf{D}\left(\mathbf{w}_T - \hat{\mathbf{w}}^{t-1}\right)\right\|_2$$

$$+ \|\mathbf{\Omega}_{T\cup\hat{T}^t}(\mathbf{I} - \mathbf{M}^*\mathbf{M})\mathbf{D}\mathbf{w}_{T^C}\|_2 + \|\mathbf{\Omega}_{T\cup\hat{T}^t}\mathbf{M}^*\mathbf{e}\|_2,$$

where the last step is due to the triangle inequality. Denote by $\mathbf{P}$ the projection onto range($[\mathbf{\Omega}_{T\cup\hat{T}^t}^*, \mathbf{D}_{T\cup\hat{T}^{t-1}}]$), which is a subspace of vectors with $4k$-sparse representations. As $\mathbf{w}_T - \hat{\mathbf{w}}^{t-1}$ is supported on $T\cup T^{t-1}$ and $\mathbf{M}$ satisfies

26

the D-RIP for $[\mathbf{\Omega}^*, \mathbf{D}]$, we have using norm inequalities and Lemma 2.3 that

$$
\begin{aligned}
\left\|\mathbf{\Omega}_{T\cup\hat{T}^t}(\mathbf{I} - \mathbf{M}^*\mathbf{M})\mathbf{D}\left(\mathbf{w}_T - \hat{\mathbf{w}}^{t-1}\right)\right\|_2 \qquad &\qquad\qquad\qquad\qquad (\text{A.4}) \\
= \left\|\mathbf{\Omega}_{T\cup\hat{T}^t}\mathbf{P}(\mathbf{I} - \mathbf{M}^*\mathbf{M})\mathbf{P}\mathbf{D}\left(\mathbf{w}_T - \hat{\mathbf{w}}^{t-1}\right)\right\|_2 \\
\leq \left\|\mathbf{\Omega}_{T\cup\hat{T}^t}\right\|_2 \left\|\mathbf{P}(\mathbf{I} - \mathbf{M}^*\mathbf{M})\mathbf{P}\right\|_2 \left\|\mathbf{D}\right\|_2 \left\|\mathbf{w}_T - \hat{\mathbf{w}}^{t-1}\right\|_2 \\
\leq \delta_{4k}\frac{B}{A}\left\|\mathbf{w}_T - \hat{\mathbf{w}}^{t-1}\right\|_2,
\end{aligned}
$$

where A and B are the frame constants and we use the fact that $\|\mathbf{D}\|_2 \leq \frac{1}{\|\mathbf{\Omega}\|_2} \leq \frac{1}{A}$ and that $\|\mathbf{\Omega}_{T\cup\hat{T}^t}\|_2 \leq \|\mathbf{\Omega}\|_2 \leq B$. Notice that when $\mathbf{\Omega}$ is tight frame, $\mathbf{\Omega}^* = \mathbf{D}$ and thus $\mathbf{\Omega}_T^* = \mathbf{D}_T$. Hence, we have δ_{3k} instead of δ_{4k} since range$([\mathbf{\Omega}_{T\cup\hat{T}^t}^*, \mathbf{D}_{T\cup\hat{T}^{t-1}}])$ is a subspace of vectors with $3k$-sparse representations.

For completing the proof we first notice that $\mathbf{w}_T - \hat{\mathbf{w}}^{t-1} = (\mathbf{w} - \hat{\mathbf{w}}^{t-1})_{T\cup\hat{T}^{t-1}}$ and that $\hat{\mathbf{w}}^{t-1}$ is the best k-term approximation of $\mathbf{w}_g^{t-1}$ in the ℓ_2 norm sense. In particular it is also the best k-term approximation of $(\mathbf{w}_g^{t-1})_{T\cup\hat{T}^{t-1}}$ and therefore $\left\|(\hat{\mathbf{w}}^{t-1} - \mathbf{w}_g^{t-1})_{T\cup\hat{T}^{t-1}}\right\|_2 \leq \left\|(\mathbf{w} - \mathbf{w}_g^{t-1})_{T\cup\hat{T}^{t-1}}\right\|_2$. Starting with the triangle inequality and then applying this fact we have

$$
\begin{aligned}
\left\|\mathbf{w}_T - \hat{\mathbf{w}}^{t-1}\right\|_2 \qquad &\qquad\qquad\qquad\qquad\qquad\qquad (\text{A.5}) \\
= \left\|(\mathbf{w} - \mathbf{w}_g^{t-1} + \mathbf{w}_g^{t-1} - \hat{\mathbf{w}}^{t-1})_{T\cup\hat{T}^{t-1}}\right\|_2 \\
\leq \left\|(\mathbf{w} - \mathbf{w}_g^{t-1})_{T\cup\hat{T}^{t-1}}\right\|_2 + \left\|(\hat{\mathbf{w}}^{t-1} - \mathbf{w}_g^{t-1})_{T\cup\hat{T}^{t-1}}\right\|_2 \\
\leq 2\left\|(\mathbf{w} - \mathbf{w}_g^{t-1})_{T\cup\hat{T}^{t-1}}\right\|_2.
\end{aligned}
$$

Combining (A.5) and (A.4) with (A.3) leads to

$$
\begin{aligned}
\left\|(\mathbf{w} - \mathbf{w}_g^t)_{T\cup\hat{T}^t}\right\|_2 \leq{}& 2\delta_{4k}\frac{B}{A}\left\|(\mathbf{w} - \mathbf{w}_g^{t-1})_{T\cup\hat{T}^{t-1}}\right\|_2 \qquad (\text{A.6}) \\
&+ \left\|\mathbf{\Omega}_{T\cup\hat{T}^t}(\mathbf{I} - \mathbf{M}^*\mathbf{M})\mathbf{D}\mathbf{w}_{T^C}\right\|_2 \\
&+ \left\|\mathbf{\Omega}_{T\cup\hat{T}^t}\mathbf{M}^*\mathbf{e}\right\|_2.
\end{aligned}
$$

It remains to bound the second term of the rhs. By using the triangle inequality and then the D-RIP with the fact that $\|\mathbf{\Omega}_{T\cup\hat{T}^t}\mathbf{D}\|_2 \leq \|\mathbf{\Omega}\mathbf{D}\|_2 \leq 1$ we have

$$
\begin{aligned}
\left\|\mathbf{\Omega}_{T\cup\hat{T}^t}(\mathbf{I} - \mathbf{M}^*\mathbf{M})\mathbf{D}\mathbf{w}_{T^C}\right\|_2 \qquad &\qquad\qquad\qquad (\text{A.7}) \\
\leq \left\|\mathbf{\Omega}_{T\cup\hat{T}^t}\mathbf{D}\mathbf{w}_{T^C}\right\|_2 + \left\|\mathbf{\Omega}_{T\cup\hat{T}^t}\mathbf{M}^*\mathbf{M}\mathbf{D}\mathbf{w}_{T^C}\right\|_2 \\
\leq \left\|\mathbf{w}_{T^C}\right\|_2 + \sqrt{1 + \delta_{2k}}\left\|\mathbf{M}\mathbf{D}\mathbf{w}_{T^C}\right\|_2 \\
\leq \left\|\mathbf{w}_{T^C}\right\|_2 + \frac{1 + \delta_{2k}}{A}\left(\left\|\mathbf{w}_{T^C}\right\|_2 + \frac{1}{\sqrt{k}}\left\|\mathbf{w}_{T^C}\right\|_1\right),
\end{aligned}
$$

where the last inequality is due to Lemmas 2.2 and 2.5. The desired result is achieved by plugging (A.7) into (A.6) and using the fact that $1 + \frac{1+\delta_{2k}}{A} \leq \frac{(1+\delta_{2k})(1+A)}{A}$. $\qquad\square$

Acknowledgment

References

[1] D. L. Donoho, M. Elad, V. N. Temlyakov, Stable recovery of sparse overcomplete representations in the presence of noise, IEEE Trans. Inf. Theory 52 (1) (2006) 6–18.

[2] K. Dabov, A. Foi, V. Katkovnik, K. Egiazarian, Image denoising with block-matching and 3D filtering, in: Proc. SPIE, Vol. 6064, 2006, p. 606414.

[3] A. Danielyan, V. Katkovnik, K. Egiazarian, BM3D frames and variational image deblurring, IEEE Trans. Image Process. 21 (4) (2012) 1715–1728.

[4] R. Zeyde, M. Elad, M. Protter, On single image scale-up using sparse-representations, in: Proceedings of the 7th international conference on Curves and Surfaces, Springer-Verlag, Berlin, Heidelberg, 2012, pp. 711–730.

[5] A. Fannjiang, T. Strohmer, P. Yan, Compressed remote sensing of sparse objects, SIAM Journal on Imaging Sciences 3 (3) (2010) 595–618.

[6] M. Lustig, D. Donoho, J. Santos, J. Pauly, Compressed sensing MRI, IEEE Signal Processing Magazine 25 (2) (2008) 72–82.

[7] J. Salmon, Z. Harmany, C.-A. Deledalle, R. Willett, Poisson noise reduction with non-local PCA, Journal of Mathematical Imaging and Vision (2013) 1–16.

[8] A. M. Bruckstein, D. L. Donoho, M. Elad, From sparse solutions of systems of equations to sparse modeling of signals and images, SIAM Review 51 (1) (2009) 34–81.

[9] M. Elad, P. Milanfar, R. Rubinstein, Analysis versus synthesis in signal priors, Inverse Problems 23 (3) (2007) 947–968.

[10] S. Nam, M. Davies, M. Elad, R. Gribonval, The cosparse analysis model and algorithms, Appl. Comput. Harmon. Anal. 34 (1) (2013) 30 – 56.

[11] E. J. Candès, Y. C. Eldar, D. Needell, P. Randall, Compressed sensing with coherent and redundant dictionaries, Appl. Comput. Harmon. Anal 31 (1) (2011) 59 – 73.

[12] S. Vaiter, G. Peyre, C. Dossal, J. Fadili, Robust sparse analysis regularization, IEEE Trans. Inf. Theory 59 (4) (2013) 2001–2016.

[13] E. J. Candès, T. Tao, Near-optimal signal recovery from random projections: Universal encoding strategies?, IEEE Trans. Inf. Theory 52 (12) (2006) 5406 –5425.

[14] E. Candès, T. Tao, Decoding by linear programming, IEEE Trans. Inf. Theory 51 (12) (2005) 4203 – 4215.

[15] E. Candès, T. Tao, The Dantzig selector: Statistical estimation when p is much larger than n, Annals Of Statistics 35 (6) (2007) 2313–2351.

[16] P. Bickel, Y. Ritov, A. Tsybakov, Simultaneous analysis of lasso and dantzig selector, Annals of Statistics 37 (4) (2009) 1705–1732.

[17] R. Giryes, M. Elad, RIP-based near-oracle performance guarantees for SP, CoSaMP, and IHT, IEEE Trans. Signal Process. 60 (3) (2012) 1465–1468.

[18] Z. T. Harmany, R. F. Marcia, R. M. Willett, This is SPIRAL-TAP: Sparse poisson intensity reconstruction algorithms – theory and practice, IEEE Trans. Img. Proc. 21 (3) (2012) 1084–1096.

[19] M. Soltanolkotabi, E. Elhamifar, E. J. Candès, Robust subspace clustering, Annals Of Statistics 42 (2) (2014) 669–699.

[20] R. Giryes, M. Elad, Sparsity-based poisson denoising with dictionary learning, IEEE Trans. Img. Proc. 23 (12) (2014) 5057–5069.

[21] R. Giryes, M. Elad, A. Bruckstein, Sparsity based methods for over-parameterized variational problems, http://arxiv.org/abs/1405.4969 (2014).

[22] Y. Pang, Z. Ji, P. Jing, X. Li, Ranking graph embedding for learning to rerank, Neural Networks and Learning Systems, IEEE Transactions on 24 (8) (2013) 1292–1303.

[23] Y. Pang, S. Wang, Y. Yuan, Learning regularized lda by clustering, IEEE Trans. Neural Networks and Learning Systems 25 (12) (2014) 2191–2201.

[24] Y. Pang, X. Li, Y. Yuan, Robust tensor analysis with l1-norm, IEEE Trans. Circuits and Systems for Video Technology 20 (2) (2010) 172–178.

[25] E. Candès, Modern statistical estimation via oracle inequalities, Acta Numerica 15 (2006) 257–325.

[26] G. Davis, S. Mallat, M. Avellaneda, Adaptive greedy approximations, Journal of Constructive Approximation 50 (1997) 57–98.

[27] L. I. Rudin, S. Osher, E. Fatemi, Nonlinear total variation based noise removal algorithms, Phys. D 60 (1-4) (1992) 259–268.

[28] D. Needell, R. Ward, Stable image reconstruction using total variation minimization, SIAM Journal on Imaging Sciences 6 (2) (2013) 1035–1058.

[29] R. Giryes, Sampling in the analysis transform domain, To Appear in Applied and Computational Harmonic AnalysisHttp://arxiv.org/abs/1410.6558.

[30] S. Chen, S. A. Billings, W. Luo, Orthogonal least squares methods and their application to non-linear system identification, International Journal of Control 50 (5) (1989) 1873–1896.

[31] S. Mallat, Z. Zhang, Matching pursuits with time-frequency dictionaries, IEEE Trans. Signal Process. 41 (1993) 3397–3415.

[32] Y. Pati, R. Rezaiifar, P. Krishnaprasad, Orthonormal matching pursuit : recursive function approximation with applications to wavelet decomposition, in: Proceedings of the 27th Annual Asilomar Conf. on Signals, Systems and Computers, 1993, pp. 40 – 44.

[33] D. Needell, J. Tropp, CoSaMP: Iterative signal recovery from incomplete and inaccurate samples, Appl. Comput. Harmon. A. 26 (3) (2009) 301 – 321.

[34] W. Dai, O. Milenkovic, Subspace pursuit for compressive sensing signal reconstruction, IEEE Trans. Inf. Theory 55 (5) (2009) 2230 –2249.

[35] T. Blumensath, M. Davies, Iterative hard thresholding for compressed sensing, Appl. Comput. Harmon. Anal 27 (3) (2009) 265 – 274.

[36] S. Foucart, Hard thresholding pursuit: an algorithm for compressive sensing, SIAM J. Numer. Anal. 49 (6) (2011) 2543–2563.

[37] T. Peleg, M. Elad, Performance guarantees of the thresholding algorithm for the cosparse analysis model, IEEE Trans. Inf. Theory 59 (3) (2013) 1832–1845.

[38] R. Giryes, S. Nam, M. Elad, R. Gribonval, M. Davies, Greedy-like algorithms for the cosparse analysis model, Linear Algebra and its Applications 441 (0) (2014) 22 – 60, special issue on sparse approximate solution of linear systems.

[39] T. Zhang, Sparse recovery with orthogonal matching pursuit under RIP, IEEE Trans. Inf. Theory 57 (9) (2011) 6215 –6221.

[40] S. Foucart, Sparse recovery algorithms: sufficient conditions in terms of restricted isometry constants, in: Approximation Theory XIII, Springer Proceedings in Mathematics, 2010, pp. 65–77.

[41] T. Cai, L. Wang, G. Xu, New bounds for restricted isometry constants, IEEE Trans. Inf. Theory 56 (9) (2010) 4388–4394.

[42] Z. Ben-Haim, Y. Eldar, M. Elad, Coherence-based performance guarantees for estimating a sparse vector under random noise, IEEE Trans. Signal Process. 58 (10) (2010) 5030 –5043.

[43] Y. Liu, T. Mi, S. Li, Compressed sensing with general frames via optimal-dual-based l1-analysis, IEEE Trans. Inf. Theory 58 (7) (2012) 4201–4214.

[44] M. Kabanava, H. Rauhut, Analysis l_1-recovery with frames and Gaussian measurements, http://arxiv.org/abs/1306.1356 (2014).

[45] T. Blumensath, Sampling and reconstructing signals from a union of linear subspaces, IEEE Trans. Inf. Theory 57 (7) (2011) 4660–4671.

[46] M. Davenport, D. Needell, M. Wakin, Signal space CoSaMP for sparse recovery with redundant dictionaries, IEEE Trans. Inf. Theory. 59 (10) (2013) 6820–6829.

[47] R. Giryes, M. Elad, Can we allow linear dependencies in the dictionary in the synthesis framework?, in: IEEE International Conference on Acoustics, Speech and Signal Processing (ICASSP), 2013, pp. 5459 – 5463.

[48] R. Giryes, M. Elad, OMP with highly coherent dictionaries, in: 10th Int. Conf. on Sampling Theory Appl. (SAMPTA), 2013, pp. 9–12.

[49] R. Giryes, M. Elad, Iterative hard thresholding for signal recovery using near optimal projections, in: 10th Int. Conf. on Sampling Theory Appl. (SAMPTA), 2013, pp. 212–215.

[50] R. Giryes, D. Needell, Greedy signal space methods for incoherence and beyond, Appl. Comput. Harmon. Anal.To appear.

[51] R. Giryes, D. Needell, Near oracle performance and block analysis of signal space greedy methods, CoRR abs/1402.2601.

[52] A. M. Tillmann, R. Gribonval, M. E. Pfetsch, Projection onto the cosparse set is NP-hard, in: IEEE International Conference on Acoustics, Speech and Signal Processing (ICASSP), 2014, pp. 7148 – 7152.

[53] R. Giryes, Y. Plan, R. Vershynin, On the effective measure of dimension in analysis cosparse models, http://arxiv.org/abs/1410.0989 (2014).

[54] E. H. Moore, On the reciprocal of the general algebraic matrix, Bulletin of the American Mathematical Society 26 (1920) 394–395.

[55] B. Ophir, M. Lustig, M. Elad, Multi-scale dictionary learning using wavelets, IEEE Journal of Selected Topics in Signal Processing 5 (5) (2011) 1014–1024.

[56] S. Ravishankar, Y. Bresler, MR image reconstruction from highly undersampled k-space data by dictionary learning, IEEE Trans. Medical Imaging 30 (5) (2011) 1028–1041.

[57] S. Ravishankar, Y. Bresler, Sparsifying transform learning for compressed sensing MRI, in: IEEE 10th International Symposium on Biomedical Imaging (ISBI), 2013, pp. 17–20.

[58] A. Kyrillidis, V. Cevher, Recipes on hard thresholding methods, in: 4th Int. Workshop on Computational Advances in Multi-Sensor Adaptive Processing (CAMSAP), 2011, pp. 353 –356.

[59] V. Cevher, An ALPS view of sparse recovery, in: IEEE International Conference on Acoustics, Speech and Signal Processing (ICASSP), 2011, pp. 5808–5811.

[60] S. Nam, M. Davies, M. Elad, R. Gribonval, Recovery of cosparse signals with greedy analysis pursuit in the presence of noise, in: 4th IEEE International Workshop on Computational Advances in Multi-Sensor Adaptive Processing (CAMSAP), 2011, pp. 361–364.

[61] D. L. Donoho, J. Tanner, Counting faces of randomly-projected polytopes when the projection radically lowers dimension, J. of the AMS 22 (1) (2009) 1–53.

[62] M. Lustig, D. L. Donoho, J. Pauly, Sparse MRI: The application of compressed sensing for rapid MR imaging, Magnetic resonance in medicine 58 (6) (2007) 1182–1195.